JOURNAL OF SOLID STATE CHEMISTRY 65, 156–167 (1986)

Luminescence of Sb^{3+} in Rare Earth Orthoborates $LnBO_3$ (Ln = Sc, Y, La, Gd, Lu)

E. W. J. L. OOMEN,* L. C. G. VAN GORKOM, W. M. A. SMIT, AND G. BLASSE

Physical Laboratory, Solid State Department, State University, P.O. Box 80.000, 3508 TA Utrecht, The Netherlands

Received November 11, 1985; in revised form February 17, 1986

The luminescence of several Sb^{3+}-activated rare earth orthoborates ($LnBO_3$–Sb^{3+}; Ln = Sc, Y, La, Gd, Lu) are reported. In all compositions the Stokes shift of the Sb^{3+} luminescence is rather large, resulting in rather low quenching temperatures (200 K or lower). The Stokes shift appears to be dependent on the coordination number and on the radius of the host lattice cation. This is explained from the assumed tendency of the Sb^{3+} ion to occupy an off-center position which becomes more apparent when the space available for the Sb^{3+} ion increases. The present results are compared with those on $LnBO_3$–Bi^{3+}. It appears that the Stokes shift of the Bi^{3+} luminescence is more sensitive to the host lattice and is smaller than the Stokes shift of the Sb^{3+} luminescence. This is explained by the large radius of the Bi^{3+} ion compared to the Sb^{3+} ion. In $GdBO_3$–Sb^{3+} thermally activated energy transfer is observed from Gd^{3+} to Sb^{3+}.

1. Introduction

It is well known that the luminescence properties of s^2 ions depend strongly on the host lattice (see, e.g., Refs. (*1–4*)). In this paper we report on the luminescence of the $5s^2$ ion Sb^{3+} in several rare earth orthoborates. Many investigations have been performed on the Sb^{3+} luminescence in oxidic systems (see, e.g., Refs. (*1–8*)), but so far no systematic investigations are known. The present results form part of such a systematic study of the luminescence of the Sb^{3+} ion in inorganic systems (see, e.g., Refs. (*9, 10*)).

The luminescence of the $6s^2$ ion Bi^{3+} in $LnBO_3$ (Ln = Sc, Y, La, Gd, Lu) at room temperature has been reported by Blasse and Bril (*11*). Recently, these measurements were extended to low temperatures while also decay times were measured (*12*). From these studies it became clear that the luminescence of the Bi^{3+} ion in $LnBO_3$ depends dramatically on the nature of the Ln^{3+} ion. It appeared that the Stokes shift of the luminescence of the Bi^{3+} ion increases with increasing host lattice cation radius (i.e., with increasing space available for the Bi^{3+} ion). This relationship is also found in several other systems, e.g., Sb^{3+} in Cs_2NaMCl_6 (M = Sc, Y, La) (*10*) and Bi^{3+} in $LiLnO_2$ and $NaLnO_2$ (Ln = Sc, Y, La, Gd, Lu) (*13*). A possible explanation for this behavior is based on the assumption that the s^2 ion tends to occupy an off-center position with regard to the surrounding li-

* To whom correspondence should be addressed.

0022-4596/86 $3.00

TABLE I

STRUCTURAL DATA OF SOME ORTHOBORATE LATTICES AND Sb^{3+} LUMINESCENCE DATA IN THOSE LATTICES (AT ROOM TEMPERATURE)

Composition	Structural data			Sb^{3+} luminescence data		
	Host cation radius (Å)[a]	Crystal structure[b]	Coordination number[b]	Lower excitation maximum (cm^{-1})	Emission maximum (cm^{-1})	Stokes shift (cm^{-1})
$ScBO_3$–Sb^{3+}	0.745	Calcite	6	32,700	24,800	7,900
$LuBO_3$–Sb^{3+}(hT)	0.861	Calcite	6	33,400	22,700	10,700
$LuBO_3$–Sb^{3+}(1T)	0.861(6-co.)	YBO_3	6	38,000[c]	23,500[c]	14,500[c]
YBO_3–Sb^{3+}	0.900(6-co.)	YBO_3	6 + 6′	36,500[c]	20,500[c]	16,000[c]
$GdBO_3$–Sb^{3+}	0.938(6-co.)	YBO_3				
$LaBO_3$–Sb^{3+}	1.216	Aragonite	9	42,000	22,500	19,500

[a] Ref. (27).
[b] Refs. (15, 17).
[c] These values are averages of the data given in Table III.

gands. This effect becomes more pronounced in host lattices in which the dopant ion replaces large cations (14).

In this paper we report on the Sb^{3+} luminescence in several orthoborates ($LnBO_3$) with different coordination number of the trivalent cation. $ScBO_3$ and the high-temperature modification of $LuBO_3$ (hereafter denoted as $LuBO_3$(hT)) adopt the calcite structure (15, 16). In this structure the trivalent cation is octahedrally coordinated.

The low-temperature modification of $LuBO_3$ (hereafter denoted as $LuBO_3$(1T)), YBO_3 and $GdBO_3$ adopt a structure which is related to the vaterite structure, the so-called YBO_3 structure (15, 17). In this structure two different sites are available for the Ln^{3+} ion, viz., an octahedrally coordinated site (6 coordination) and a 12-coordinated site (6 + 6′ coordination). The latter site consists of six oxygen ligands at the same distance from the cation and six oxygen ligands at a slightly longer distance from the cation. The Ln^{3+}–O^{2-} distances for the 12-coordinated site are about 16% larger than those of the 6-coordinated site (17). The concentration ratio of the octahedral sites to the 12-coordinated sites is 2 : 1.

The compound $LaBO_3$ has the aragonite structure (15, 16). In this structure the La^{3+} ion is coordinated by nine oxygen ions. The structural data and the ionic radii of the Ln^{3+} ions are gathered in Table I.

2. Experimental

2.1. Sample preparation. Starting materials were Sc_2O_3, Y_2O_3, Lu_2O_3 (Highways International 99.99%), Gd_2O_3, La_2O_3 (Highways International 99.999%), Sb_2O_3, and H_3BO_3 (Merck, p.a.). To prepare the borates with the calcite and YBO_3 structure, the rare earth oxides and Sb_2O_3 were dissolved in diluted (5 *M*) hydrochloric acid (Baker, p.a.). By adding boric acid to this solution (in an excess of 20%) a white precipitate was obtained. After washing, the precipitate was fired in air in a platinum crucible at 1100°C during 1½ hr, except Lu BO_3(1T) which was fired in air at 700°C during 2½ hr. $LaBO_3$–Sb^{3+} was obtained by grinding La_2O_3 and Sb_2O_3 and firing the mixture in air at 400°C for 2½ hr followed by a second firing period of 2½ hr at 800°C. The resulting $(La,Sb)_2O_3$ was grinded with H_3BO_3 (excess 25%) and fired in air in a

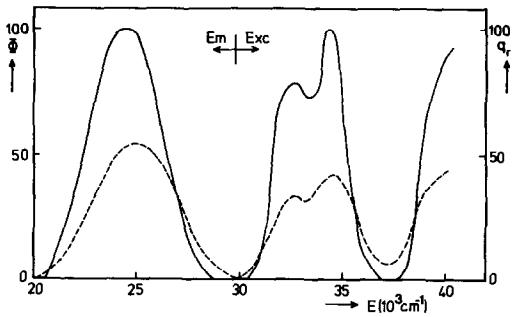

FIG. 1. Emission and excitation spectra of the luminescence of Sb^{3+} in $ScBO_3$–Sb^{3+} at LHeT (—) and at RT (---). Φ denotes the radiant power per constant energy interval in arbitrary units. q_r gives the relative quantum output in arbitrary units.

platinum crucible at 400°C for 1½ hr followed by a second firing period of 3½ hr at 600°C.

All samples obtained were white powders. They were checked by X-ray powder diffraction using Cu$K\alpha$ radiation. The actual amount of Sb in the samples was determined by atomic absorption spectroscopy. It turned out that the concentration of Sb in the final samples was considerably less than in the starting mixtures, especially for the borates fired at 1100°. For $LuBO_3$–Sb^{3+}(1T) and $LaBO_3$–Sb^{3+} the built-in amount of Sb is about 3–5% of the starting amount, for the other borates 0.1–1% (see next section for precise data on the Sb^{3+} content of the different samples).

2.2. Instrumentation. Diffuse reflectance spectra were recorded at room temperature with a Perkin Elmer Lambda 7 UV/VIS spectrophotometer. Luminescence spectra were measured using a Perkin Elmer MPF 44 B spectrofluorometer equipped with an Oxford CF 204 liquid helium flow cryostat. The excitation spectra were corrected for lamp intensity using lumogen T-rot GG as a standard. The emission spectra were corrected for the photomultiplier sensitivity. The photon flux per constant energy interval, Φ, is obtained by multiplying the radiant power per constant wavelength interval by λ^3.

Decay time measurements were performed with a photon counting system (EG & G). Details of this system are described elsewhere (*14*). The excitation source was an EG & G 108 AU Xe flash lamp (pulse width ~4 μsec). The excitation wavelength regions were selected with the use of interference and cutoff filters. The emission wavelength was selected by a double monochromator (Jobin YVON, HRD 1). For detection a photomultiplier tube (RCA C31034) was used.

3. Results

3.1. Luminescence of Sb^{3+} in Borates with the Calcite Structure

3.1.1. $ScBO_3$–Sb^{3+}. Samples containing 300 and 500 mole ppm Sb were investigated. The spectral data for both samples were similar. In the diffuse reflectance spectrum two bands are observed, viz., a strong one at 250 nm and a weaker one at 280 nm. The 250-nm band shows a shoulder at the short wavelength side, indicating that this band may be split into a doublet. No conclusions were possible about the shape of the 280-nm band because of interference with host lattice absorption. The excitation and emission spectra of $ScBO_3$–Sb^{3+} at liquid helium temperature (LHeT) and at room temperature (RT) are given in Fig. 1. The lower intensities at RT are due to temperature quenching which starts above 200 K. The excitation spectrum consists of two bands, a doublet band around 34,000 cm^{-1} (~290 nm) and a band with its maximum around 40,000 cm^{-1} (~250 nm). The shape of the latter band could not be measured accurately because of the low intensity of the Xe lamp in this wavelength region. Moreover, the observed value for the integrated intensity ratio of the two excitation bands is at fault. In the reflectance spec-

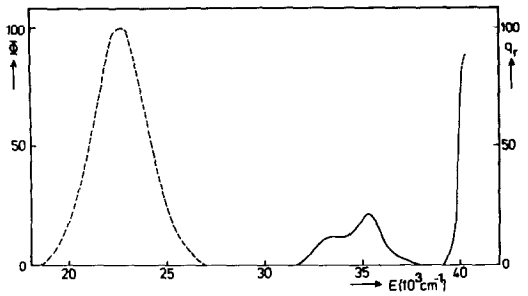

FIG. 2. Emission (---) and excitation (—) spectra of $LuBO_3$–Sb^{3+} (hT) at LHeT. Φ denotes the radiant power per constant energy interval in arbitrary units. q_r gives the relative quantum output in arbitrary units.

trum the 250-nm band is much stronger than the 290-nm band in accordance with the assignment (see Section 4), viz., 250 nm: $^1S_0 \rightarrow {}^1P_1$ (allowed transition), 290 nm: $^1S_0 \rightarrow {}^3P_1$ (spin-orbit allowed transition). The weak Xe lamp output in the region of the strong absorption band ($^1P_1$) as compared to the considerably higher output in the region of the weaker band ($^3P_1$) leads to incomplete excitation of the $^1S_0 \rightarrow {}^1P_1$ transition, causing a far too low $^1P_1 : {}^3P_1$ intensity ratio. Only for very low Sb^{3+} concentrations this problem vanishes (*18*). The only emission band is broad and has its maximum at about 24,800 cm^{-1} (~405 nm).

3.1.2. $LuBO_3$–Sb^{3+} (hT). Samples containing about 20, 40, and 60 mole ppm Sb^{3+} were studied. The spectral data turned out to be independent of the Sb^{3+} concentration. The diffuse reflectance spectrum contains a strong absorption band at about 235 nm and a weaker one at 278 nm. The 235-nm band has a doublet structure with maxima at 228 and 243 nm. The excitation and emission spectra of $LuBO_3$–Sb^{3+} at LHeT are given in Fig. 2. The temperature quenching of the luminescence shows the same behavior as that of $ScBO_3$–Sb^{3+}. The excitation spectrum consists of two bands, a doublet around 34,500 cm^{-1} (~290 nm) and a band with its maximum around 41,000 cm^{-1} (~245 nm). Again, the shape of the latter band could only be roughly determined because of instrumental limitations. The only emission band is broad and has its maximum at 22,600 cm^{-1} (~440 nm).

3.1.3. Decay time measurements. For $ScBO_3$–Sb^{3+} and $LuBO_3$–Sb^{3+} (hT) the decay curves were exponential at all temperatures. Figures 3 and 4 show the decay times as a function of temperature for $ScBO_3$–Sb^{3+} and $LuBO_3$–Sb^{3+} (hT).

These results were analyzed with the use of a three level scheme (see insert, Fig. 3) (*19, 20*). Levels 0, 1, and 2 represent the $^1S_0$ ground state and the $^3P_0$ and $^3P_1$ excited states of the Sb^{3+} ion discussed in Section 4. Excitation occurs into level 2. After excitation at low temperatures three processes are taken into account: the radiative transition from level 2 to level 0 (probability k_{20}), the nonradiative transition from level 2 to level 1 (probability k_{21}) and the radiative transition from level 1 to level 0 (probability k_{10}). If $k_{21} \gg k_{20}$, level 1 is the only emitting level at low temperatures. The probability of thermal population of level 2 from level 1 (k_{12}) becomes important at higher temperatures and is given by

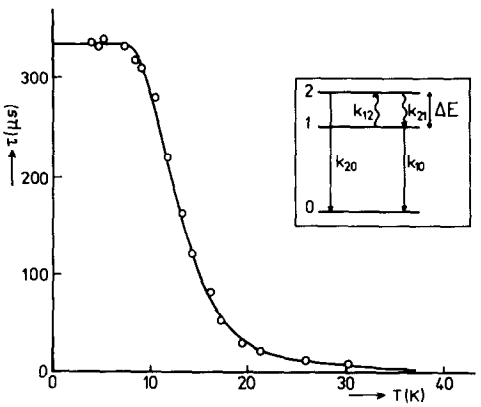

FIG. 3. Decay times of the 24,500-cm^{-1} emission of $ScBO_3$–Sb^{3+} as a function of temperature. The drawn line gives the best fit of the data to Eq. (2). The insert shows the three-level diagram (see text).

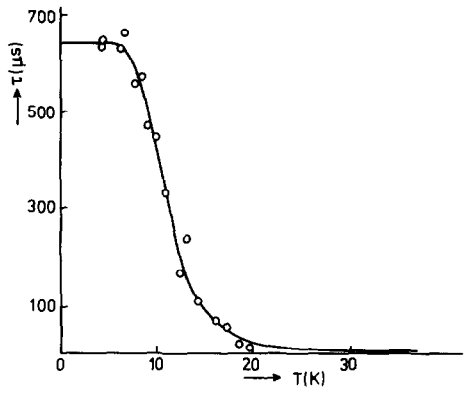

FIG. 4. Decay times of the 22,600-cm^{-1} emission of $LuBO_3$–Sb^{3+} (hT) as a function of temperature. The drawn line gives the best fit of the data to Eq. (2).

$$k_{12} = k_{21} \exp\left(\frac{-\Delta E}{kT}\right) \qquad (1)$$

where ΔE denotes the energy difference between levels 1 and 2. Since for an s^2 ion $k_{20} \gg k_{10}$, only emission from level 2 will be observed at higher temperatures. The temperature dependence of the decay time can be expressed as (*19, 20*)

$$\frac{1}{\tau} = \frac{k_{10} + k_{20} \exp\left(\frac{-\Delta E}{kT}\right)}{1 + \exp\left(\frac{-\Delta E}{kT}\right)}. \qquad (2)$$

The values of k_{10} can be obtained from the low-temperature decay time ($\tau_1 = k_{10}^{-1}$). Fitting the measured decay times to Eq. (2) yields values for $k_{20} = \tau_2^{-1}$ and ΔE. The best fits of the experimental data to Eq. (2) correspond to the full lines in Figs. 3 and 4. The resulting decay parameters are given in Table II.

3.2. Luminescence of Sb^{3+} in Borates with the YBO_3 Structure

3.2.1. $LuBO_3$–Sb^{3+} (1T). The investigated samples contained 1000, 1700, and 2000 mole ppm Sb. The spectra were independent of the Sb concentration. The diffuse reflectance spectra showed a broad intense band around 215 nm and a weaker band around 250 nm. Figure 5 gives the excitation and emission spectra of $LuBO_3$–Sb^{3+} (1T) at LHeT. The observed emission consists of a broad band between 18,000 and 28,000 cm^{-1}. Closer examination of the form of the emission band as a function of the excitation wavelength revealed that the observed emission band actually consists of two strongly overlapping bands, each with its own excitation spectrum (see Fig. 5). The shape and position of the two components of the observed emission band could be roughly determined by the above mentioned procedure and are indicated by broken lines in Fig. 5. Temperature quenching starts at about 180 K.

In view of the strong overlap of the excitation bands as well as the emission bands of both centers and because of the low emission intensities of the samples no decay time measurements could be performed.

TABLE II

SPECTRAL DATA (AT RT) AND DECAY TIME PARAMETERS OF THE Sb^{3+} LUMINESCENCE IN CALCITE-STRUCTURED BORATES

Composition	Excitation maxima $^1S_0$–$^3P_1$		Emission maximum (cm^{-1})	Stokes shift (cm^{-1})	k_{10} (sec^{-1})	k_{20} (sec^{-1})	ΔE (cm^{-1})
	Lower energy component (cm^{-1})	Higher energy component (cm^{-1})					
$ScBO_3$–Sb^{3+}	32,700	34,500	24,800	7,900	2990 ± 50	(2.5 ± 1) × 10^6	62 ± 4
$LuBO_3$–Sb^{3+}	33,400	35,300	22,700	10,700	1570 ± 30	(9 ± 3) × 10^5	48 ± 4

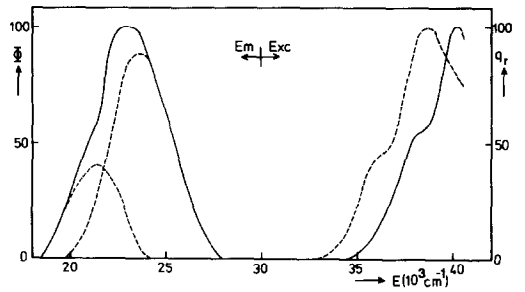

FIG. 5. Emission and excitation spectra of the luminescence of $LuBO_3$–Sb^{3+} (1T) at LHeT. The excitation spectra are recorded for emission at 26,000 cm^{-1} (—) and at 20,000 cm^{-1} (---). The emission spectrum (—) is recorded for excitation at 40,000 cm^{-1}. The broken lines in the emission spectrum represent the two emission bands (see text).

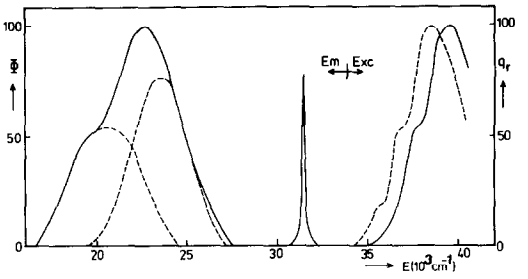

FIG. 6. Emission and excitation spectra of the luminescence of $GdBO_3$–Sb^{3+} at LHeT. The excitation spectra are recorded for emission at 25,000 cm^{-1} (—) and at 19,000 cm^{-1} (---). The emission spectrum (—) is recorded for excitation at 39,000 cm^{-1}. The broken lines in the emission spectrum represent the two emission bands. For further explanation see text.

No energy transfer between the two Sb^{3+} centers was observed in contrast to the case of Bi^{3+} in YBO_3-structured borates (*12*). This is not unexpected in view of the absence of any spectral overlap between excitation and emission bands (see Fig. 5) and the low Sb^{3+} concentration of the samples.

3.2.2. YBO_3–Sb^{3+}. The investigated samples contained about 30,100 and 150 mole ppm Sb. The spectra were independent of the Sb concentration. The diffuse reflectance spectrum is very similar to that of $LuBO_3$–Sb^{3+} (1T). The same holds for the excitation and emission spectra. The quenching temperature is about 160 K. For the same reasons as for $LuBO_3$–Sb^{3+} (1T) no decay time measurements could be performed.

3.2.3. $GdBO_3$–Sb^{3+}. The investigated sample contained 50 mole ppm Sb. The diffuse reflectance spectrum shows, apart from the Gd^{3+} peaks, a broad intense band around 215 nm and a weaker broadband around 250 nm. Figure 6 gives the emission and excitation spectra at LHeT obtained in a similar way as described for $LuBO_3$–Sb^{3+} (1T). The emission spectrum shows, in addition to the Sb^{3+} bands, a Gd^{3+} emission line at 31,500 cm^{-1} (317 nm) for broadband excitation around 40,000 cm^{-1} which excites both Sb^{3+} and Gd^{3+} ($^8S \rightarrow {}^6D$). The Gd^{3+} emission quenches rapidly at increasing temperatures and has completely vanished at 80 K. Temperature quenching of the Sb^{3+} luminescence starts around 180 K.

Figure 7 shows the uncorrected excitation spectra at LHeT and at RT of the Sb^{3+} emission at 20,000 cm^{-1}, in which several weak Gd^{3+} features are observed at about

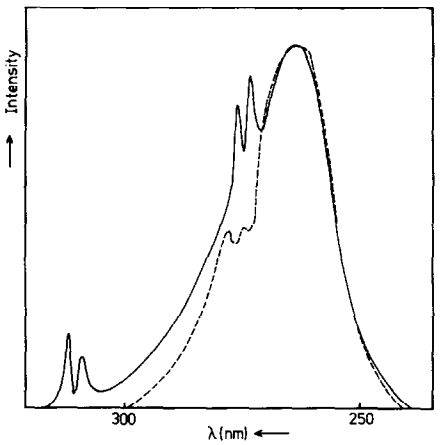

FIG. 7. *Uncorrected* excitation spectrum of the Sb^{3+} luminescence of $GdBO_3$–Sb^{3+} at LHeT (---) and at RT (—). The emission is at 20,000 cm^{-1}.

277 and 314 nm (these features are hardly discernable in the corrected spectra). At low temperatures the Gd^{3+} absorption lines appear as negative features in the Sb^{3+} excitation band. This implies that there is no transfer from Gd^{3+} to Sb^{3+} because the excitation energy absorbed by the Gd^{3+} ions is lost for Sb^{3+} emission. At higher temperatures, however, the situation changes and the Gd^{3+} absorption lines at 277 and 314 nm appear as positive features indicating thermally activated energy transfer from Gd^{3+} to Sb^{3+}. The same is observed in the excitation spectra of the Sb^{3+} emission at 25,000 cm^{-1}. The excitation spectrum of the Gd^{3+} emission contains only the characteristic Gd^{3+} absorption lines. This shows that there is no energy transfer from Sb^{3+} to Gd^{3+}.

For similar reasons as given for $LuBO_3$–Sb^{3+} (1T), decay time measurements could not be performed.

3.3. Luminescence of Sb^{3+} in a Borate with the Aragonite Structure: $LaBO_3$–Sb^{3+}

The investigated sample contained 1400 mole ppm Sb. In the diffuse reflectance spectrum a strong absorption band at 48,000 cm^{-1} (208 nm) with a weak shoulder at about 42,000 cm^{-1} (~240 nm) was observed. A reliable excitation spectrum in the wavelength region below 250 nm could not be measured due to experimental limitations. Excitation at about 240 nm yielded a weak and broad emission band around 22,500 cm^{-1} (445 nm). Temperature quenching of this band starts already at about 100 K.

4. Discussion

4.1. Sb^{3+} Luminescence in Calcite-Structured Borates ($ScBO_3$–Sb^{3+} and $LuBO_3$–Sb^{3+} (hT))

The low-temperature emission bands observed for $ScBO_3$–Sb^{3+} (Fig. 1) and $LuBO_3$–Sb^{3+} (hT) (Fig. 2) can be ascribed to the $^3P_0 \rightarrow {}^1S_0$ transition (in spite of the site symmetry of the Sb^{3+} ion we will use the free ion terms to designate the energy levels of Sb^{3+}). The rather long decay times at low temperatures clearly reflect the forbidden character of the $^3P_0 \rightarrow {}^1S_0$ transition. At increasing temperature the $^3P_1$ level becomes populated. This is confirmed by the large drop in decay time in the temperature region from 7 to 25 K (Figs. 3 and 4). The rather short decay time at temperatures above 25 K shows that the spin selection rule for the $^3P_1 \rightarrow {}^1S_0$ transition is considerably relaxed by spin-orbit coupling. The energy differences ΔE between the $^3P_0$ and $^3P_1$ levels as obtained from Eq. (2) (see Table II) cannot be obtained from the differences between the emission maxima at LHeT and RT because the maxima of the broad emission bands cannot be measured very accurately.

The diffuse reflectance spectra and the excitation spectra show two excitation bands. The high energy band is assigned to the $^1S_0 \rightarrow {}^1P_1$ transition, the low energy band to the $^1S_0 \rightarrow {}^3P_1$ transition. The $^1S_0 \rightarrow {}^1P_1$ transition is electric-dipole allowed, while the $^1S_0 \rightarrow {}^3P_1$ transition is only partly allowed by spin-orbit interaction. This explains why the high energy excitation band is the more intense one. A closer examination of the excitation spectra shows that the $^1S_0 \rightarrow {}^3P_1$ excitation band has a doublet structure. At LHeT the splitting is about 1700 cm^{-1} for $ScBO_3$–Sb^{3+} and about 1800 cm^{-1} for $LuBO_3$–Sb^{3+} (hT). No splitting could be observed for the $^1S_0 \rightarrow {}^1P_1$ transition in the excitation spectrum for reasons mentioned before. A doublet splitting shows up, however, in the diffuse reflectance spectrum (see Section 3), very clearly for $LuBO_3$–Sb^{3+} (hT), less resolved for $ScBO_3$–Sb^{3+}. There are two possible explanations for the appearance of a $^1S_0 \rightarrow {}^3P_1$ doublet in excitation.

One explanation is that we are dealing with a crystal-field splitting of the $^3P_1$ level.

The site symmetry of the trivalent ion (and hence the Sb^{3+} ion) in calcite structured orthoborates is S_6. The $^3P_1$ level splits, under S_6 symmetry, into a ^3E_u level and a $^3A_{1u}$ level. This was observed for Bi^{3+} in $ScBO_3$ and $LuBO_3$ (hT) (*12*).

The other explanation is that the structure of the excitation band is due to the Jahn-Teller effect. This effect is well known for monovalent s^2 ions in alkali halides (see, e.g., Refs. (*21–23*)). Coupling of the electronic levels with lattice vibrations yields a doublet structure for the $^1S_0 \rightarrow {}^3P_1$ transition. For Sb^{3+} this has been observed in MgS (*24*), CaS (*25*), and Cs_2NaMCl_6 (with M = Sc, Y, La) (*10, 18*).

However, the following reasons strongly suggest that in the present case the observed splitting is caused by the crystal field and not by Jahn-Teller interaction.

(i) From LHeT to RT the intensity ratio of the doublet components does not change. This is what we expect for a crystal-field splitting, while in case of a Jahn-Teller interaction a clear change of the intensity ratio should be observed (*18, 21–23*).

(ii) From LHeT to RT only a small increase of the splitting is observed (about 100 cm^{-1}). If the splitting is due to a Jahn-Teller interaction, a much more pronounced increase of the splitting would be expected (*18, 21, 22, 24*).

(iii) When the structure is due to the Jahn-Teller effect, the $^1S_0 \rightarrow {}^1P_1$ excitation band must be split into a triplet (*18, 21–25*), whereas the diffuse reflectance spectra for $ScBO_3$–Sb^{3+} and $LuBO_3$–Sb^{3+} (hT) show a doublet structure. This may be compared to the $^1S_0 \rightarrow {}^1P_1$ excitation band of Sb^{3+} in the cubic elpasolite lattice Cs_2NaMCl_6 (M = Sc, Y, La), for which we observed a clear triplet structure (*18*).

In Table II the more important spectral results for $ScBO_3$–Sb^{3+} and $LuBO_3$–Sb^{3+} (hT) are collected. The Stokes shift is taken as the energy difference between the maximum of the emission band and the lower energy maximum of the $^3P_1$ excitation band. Inspection of Table I shows that the Stokes shift increases with increasing radius of the host lattice cation. This relationship has been reported before for s^2 ions in various host lattices (see, e.g., Refs. (*10, 12, 13*)). A physical basis for this phenomenon results from the assumption that the s^2 ion tends to occupy an off-center position with regard to the surrounding ligands. In the excited state the s^2 ion shifts to a more central position. This effect becomes larger if the space available for the s^2 ion in the host lattice increases, resulting in a larger Stokes shift (*14*).

It is important to note, however, that for Sb^{3+} in the calcite-structured borates the larger Stokes shift is found for the smaller ΔE (see Table II). The same relationship has been found by Blasse and Van der Steen (*26*) for Bi^{3+}-activated phosphors and has been shown to be generally valid for s^2 ions on cubic positions by Mugnai *et al.* (*27*). In such cases the theory of the Jahn-Teller quenching of the spin-orbit interaction shows ΔE to be inversely proportional to E_{JT}, the Jahn-Teller stabilization energy. Since E_{JT} may form a considerable part of the total Stokes shift, the experimentally observed correlation between ΔE and the Stokes shift becomes clear. Therefore, these observations may indicate that a pseudo-Jahn-Teller effect is present in the relaxed excited state of the Sb^{3+} ion in the calcite-structured lattices, a reasonable assumption in view of the near-cubic site symmetry (S_6). This suggests that the Jahn-Teller effect might as well be present in absorption, causing an additional splitting of the excitation bands which apparently turns out to be too small to be observed.

Finally, we note that the quenching temperature of the Sb^{3+} luminescence in calcite-structured borates is about 200 K, while for the Bi^{3+} luminescence in these compounds no temperature quenching oc-

TABLE III

SPECTRAL DATA OF THE Sb^{3+} LUMINESCENCE IN YBO_3-STRUCTURED BORATES AT ROOM TEMPERATURE[a]

Composition	Center 1			Center 2		
	Lower excitation maximum	Emission maximum	Stokes shift	Lower excitation maximum	Emission maximum	Stokes shift
$LuBO_3$–Sb^{3+}(1T)	~38,400	~23,700	~14,700	~36,700	~21,300	~15,400
YBO_3–Sb^{3+}	~37,900	~23,900	~14,000	~36,600	~20,300	~16,300
$GdBO_3$–Sb^{3+}	~38,000	~23,500	~14,500	~36,900	~20,500	~16,400

[a] All values in cm^{-1}.

curs up to room temperature (*12*). This can be related to the larger Stokes shift for the Sb^{3+} luminescence (~10,000 cm^{-1}) compared with those for the Bi^{3+} luminescence (~2000 cm^{-1}).

4.2. *Sb^{3+} Luminescence in YBO_3-Structured Borates ($LuBO_3$–Sb^{3+} (1T), YBO_3 and $GdBO_3$)*

The luminescence spectra show clearly that two luminescent centers are present, reflecting the two crystallographic sites available for the Ln^{3+} (and hence the Sb^{3+}) ion, viz., a 6 and a 6 + 6′ center (see Section 1). For all three compounds the emission of both centers is assigned to the $^3P_1 \rightarrow {}^1S_0$ transition (or to the $^3P_0 \rightarrow {}^1S_0$ transition at LHeT). The observed excitation bands are assigned to the $^1S_0 \rightarrow {}^3P_1$ transition. For similar reasons as in the case of the calcite-structured borates the doublet structure of the excitation bands is ascribed to crystal-field splitting. The fact that the splitting in YBO_3-structured borates is not smaller than in calcite-structured borates, although in the case of YBO_3 and $GdBO_3$ the space available for the Sb^{3+} ion is larger, is probably due to the off-center position of the Sb^{3+} ion, as indicated by the large Stokes shift (see below).

The main spectral data for the luminescence of Sb^{3+} in the YBO_3-type lattices are collected in Table III. The positions of the excitation and emission maxima could only roughly be estimated, since the observed features consist of overlapping bands. This implies that the presented Stokes shifts are rather inaccurate. Table III shows that the Stokes shift of Sb^{3+} on the one crystallographic site is about 14,500 cm^{-1}, while at the other site the shift amounts to about 16,000 cm^{-1}. The space available for the Sb^{3+} ion will increase in going from the 6- to the (6 + 6′)-coordinated site (*17*). Since the Stokes shift is expected to increase when the space available for the Sb^{3+} ion increases (*14*), the center with the smaller Stokes shift (center 1 in Table III) is assigned to Sb^{3+} on a 6-coordinated site and the center with the larger Stokes shift (center 2 in Table III) to Sb^{3+} on a (6 + 6′)-coordinated site. Apparently, the Stokes shift of these two centers does not depend on the radius of the host cation.

It is remarkable that for YBO_3-structured borates the luminescence of the Sb^{3+} ion is much less dependent on the host lattice than that of the Bi^{3+} ion (*12*). A possible explanation for this is the small radius of the Sb^{3+} ion (0.76 Å) compared with the Bi^{3+} ion (1.02 Å) (*28*). An inspection of the radii given in Table I reveals that the Bi^{3+} ion is larger than the host cations, while the Sb^{3+} ion is smaller (see also Section 4.4.). This suggests that for the Sb^{3+} ion the size of the sites in the YBO_3-structured borates is large enough to occupy the most favorable off-center position, even for the small-

est host lattice cation, whereas the large Bi^{3+} ion is seriously hampered by varying space limitations.

The excitation spectrum of the Sb^{3+} emission of $GdBO_3$–Sb^{3+} contains at higher temperatures also Gd^{3+} peaks (Fig. 7). This shows that thermally activated energy transfer occurs from Gd^{3+} to Sb^{3+}. This is only possible, if the Gd^{3+} emission line overlaps the Sb^{3+} excitation band. At LHeT this is not the case. At RT, however, the Sb^{3+} excitation bands are just broad enough to be overlapped slightly by the $^6P \rightarrow {}^8S$ transition of Gd^{3+}, so that energy transfer from Gd^{3+} to Sb^{3+} can take place.

We are now able to interpret the transfer phenomena in $GdBO_3$–Sb^{3+}, neglecting the (small) difference between the spectral characteristics of the Sb^{3+} ion at the two different sites.

(i) Transfer from Sb^{3+} to Gd^{3+} never takes place because of the strong relaxation in the Sb^{3+} excited state which brings the relaxed excited state far out of resonance with even the lowest Gd^{3+} level. The same observation was made by Hao and Blasse for GdB_3O_6–Sb^{3+} (*4*).

(ii) Excitation of the Gd^{3+} ion at low temperatures results in energy migration within the Gd^{3+} sublattice. The migrating energy is trapped by Gd^{3+} traps from where emission occurs (*4, 29*). The fast decrease of the Gd^{3+} trap intensity with increasing temperature is due to detrapping; the excitation energy is now trapped by killer centres. At still higher temperatures, however, $Gd^{3+} \rightarrow Sb^{3+}$ transfer becomes possible, the Sb^{3+} ions start to trap the migrating Gd^{3+} excitation energy and Sb^{3+} emission is observed. In fact the Gd^{3+} lines in the Sb^{3+} excitation spectrum are observed for temperatures above 100 K. The Gd^{3+} trap emission is completely quenched at that temperature. The $Gd^{3+} \rightarrow Sb^{3+}$ transfer can be rather efficient in spite of the small spectral overlap, because the absorption strength of the Sb^{3+} transition is by no means low. A rough estimate of the critical distance (R_c) for this transfer can be obtained as follows. In the formula for R_c (*30*),

$$R_c^6 = 0.6 \times 10^{28} \frac{Q_{Sb^{3+}}}{E^4} \text{ SO}. \qquad (3)$$

we take for the absorption cross section $Q_{Sb^{3+}} = 10^{-17}$ cm².eV (*31*); for E, the energy of the maximal spectral overlap ~4 eV (~315 nm); and for the spectral overlap (SO) 2×10^{-3} eV^{-1} as estimated from the room temperature spectral data. This yields for R_c nearly 9 Å. Since the spectral overlap will decrease with decreasing temperature, also R_c will decrease, so that at a certain temperature (obviously below 100 K) the transfer probability will vanish.

4.3. Sb^{3+} Luminescence in an Aragonite-Structured Borate: $LaBO_3$–Sb^{3+}

Although the results on $LaBO_3$–Sb^{3+} are rather poor and inaccurate, they are, nevertheless, illustrative in the present context.

The emission (~445 nm) is assigned to the $^3P_1 \rightarrow {}^1S_0$ transition (or the $^3P_0 \rightarrow {}^1S_0$ transition at low temperatures). The intense band at 208 nm in the diffuse reflectance spectrum is assigned to the $^1S_0 \rightarrow {}^1P_1$ transition, the weaker band at about 240 nm to the partly allowed $^1S_0 \rightarrow {}^3P_1$ transition. This results in a large Stokes shift of about 19,500 cm^{-1}. However, this value is very inaccurate.

This large Stokes shift is expected because the La^{3+} ion is the largest host lattice cation in the orthoborates (see Table I) and it is surrounded by nine oxygen ions. The space available for the Sb^{3+} ion is comparable to the 12-coordinated site in the YBO_3-structured host lattices, however, the La^{3+}–O^{2-} distance show a large spread of about 0.3 Å (*16*). Therefore, in contrast to the other sites, the 9-coordinated site clearly deviates from spherical symmetry. This probably reinforces the tendency to occupy an off-center position, leading to a

large Stokes shift. The rather low quenching temperature is a direct consequence of the large Stokes shift.

4.4. General Discussion

Table I gives an overview of the Sb^{3+} luminescence data in the orthoborate lattices and the structural data of these lattices. It shows that the Stokes shift increases with increasing space available (corresponding, except for the YBO_3-type lattices, to the radius of the host lattice cation) and increasing coordination number. Assuming that the Sb^{3+} ion tends to occupy an off-center position in its ground state, shifting to a more central position in the excited state, the data of Table I suggest that the actual off-center position is determined both by the coordination of the Sb^{3+} ion as well as by the space available for the dopant ion, as reflected by the radius of the host lattice cation.

A comparison with Bi^{3+} in the same host lattices reveals that the Bi^{3+} luminescence is more sensitive to changes in space and coordination of the host lattice cation site. The Stokes shift of the Sb^{3+} luminescence varies only with a factor 2.5 by going from $ScBO_3$–Sb^{3+} to $LaBO_3$–Sb^{3+} (Table I), while for the Bi^{3+} luminescence the Stokes shift varies with a factor 5 (from 1800 cm^{-1} for $ScBO_3$–Bi^{3+} to 9300 cm^{-1} for $LaBO_3$–Bi^{3+}) (*12*). Presumably, this results from the relative large radius of the Bi^{3+} ion (1.02 Å) in comparison with that of the Sb^{3+} ion (0.76 Å) (*28*), leading to a tight position for Bi^{3+} in all but the aragonite lattices. Therefore, a stronger influence of the lattice on the Bi^{3+} luminescence than on the Sb^{3+} luminescence has to be expected. It is of interest to note that in the YBO_3-structured lattices the Sb^{3+} Stokes shift is (almost) independent of the host cation radius, while the Bi^{3+} Stokes shift shows a clear dependence (*12*), indicating that changes in the available space become more important in cases in which the radius of the dopant ion is larger than that of the host lattice cation.

Furthermore, the excitation energies of Table I show a tendency to increase in going from $ScBO_3$–Sb^{3+} to $LaBO_3$–Sb^{3+}. This might suggest a correlation between the excitation energy and the off-center position of the Sb^{3+} ion. This is a subject of further study.

Acknowledgments

The authors are indebted to Mr. H. W. van Westerveld for carrying out part of the experimental work and to Mr. G. J. Dirksen for performing the atomic absorption measurements.

References

1. G. Blasse and A. Bril, *J. Chem. Phys.* **47,** 1920 (1967).
2. G. Blasse, *Chem. Phys. Lett.* **104,** 160 (1984).
3. G. Blasse and G. J. Dirksen, *Phys. Status Solidi B* **110,** 487 (1982).
4. Hao Zhiran and G. Blasse, *Mat. Chem. Phys.* **12,** 257 (1985).
5. T. S. Davis, E. R. Kreidler, and T. F. Soules, *J. Luminescence* **4,** 48 (1971).
6. J. Grafmeyer, J. C. Bourcet, and J. Janin, *J. Luminescence* **11,** 369 (1976).
7. K. H. Butler, "Fluorescent Lamp Phosphors: Technology and Theory," Pennsylvania State Univ. Press, State College, 1980.
8. J. Th. W. de Hair and W. L. Konijnendijk, *J. Electrochem. Soc.* **127,** 161 (1980).
9. E. W. J. L. Oomen, W. M. A. Smit, and G. Blasse, *Chem. Phys. Lett.* **112,** 547 (1984).
10. E. W. J. L. Oomen and G. J. Dirksen, *Mat. Res. Bull.* **20,** 453 (1985).
11. G. Blasse and A. Bril, *J. Chem. Phys.* **48,** 217 (1968).
12. A. Wolfert, E. W. J. L. Oomen, and G. Blasse, *J. Luminescence* **31, 32,** 308 (1984); *J. Solid State Chem.* **59,** 280 (1985).
13. A. C. van der Steen, J. J. P. van Hesteren, and A. P. Slok, *J. Electrochem. Soc.* **128,** 1327 (1981).
14. C. W. M. Timmermans and G. Blasse, *J. Solid State Chem.* **52,** 222 (1984).
15. R. W. G. Wyckoff, "Crystal Structures," Vol. II, Wiley, New York, 1963.

16. R. E. NEWNHAM, M. J. REDMAN, AND R. P. SANTORO, *J. Am. Ceram. Soc.* **46,** 253 (1963).
17. W. F. BRADLEY, D. L. GRAF, AND A. S. ROTH, *Acta Crystallogr.* **20,** 283 (1966).
18. E. W. J. L. OOMEN, W. M. A. SMIT, AND G. BLASSE, *J. Phys. C* **19,** 3263 (1986).
19. A. E. HUGHES AND G. P. PELLS, *Phys. Status Solidi B* **71,** 707 (1975).
20. G. BOULON, C. PEDRINI, M. GUIDONI, AND CH. PANNEL, *J. Phys.* **36,** 267 (1975).
21. Y. TOYOZAWA AND M. INOUE, *J. Phys. Soc. Jpn.* **21,** 1663 (1966).
22. A. FUKUDA, S. MAKISHIMA, T. MABUCHI, AND R. ONAKA, *J. Chem. Phys. Solids* **28,** 1763 (1967).
23. A. RANFAGNI, D. MUGNAI, M. BACCI, G. VILIANI, AND M. P. FONTANA, *Adv. Phys.* **2,** 823 (1983).
24. S. ASANO AND N. YAMASHITA, *J. Phys. Soc. Jpn.* **49,** 2231 (1980).
25. N. YAMASHITA, *J. Phys. Soc. Jpn.* **35,** 1039 (1973).
26. G. BLASSE AND A. C. VAN DER STEEN, *Solid State Commun.* **31,** 993 (1979).
27. D. MUGNAI, A. RANFAGNI, O. PILLA, G. VILIANI, AND M. MONTAGNA, *Solid State Commun.* **35,** 975 (1980).
28. R. D. SHANNON, *Acta Crystallogr. Sect. A* **32,** 751 (1976).
29. A. J. DE VRIES AND G. BLASSE, *J. Phys.* **46,** 109 (1985).
30. G. BLASSE, *Philips Res. Rep.* **24,** 131 (1969).
31. C. K. JØRGENSEN, "Absorption Spectra and Chemical Bonding in Complexes," Pergamon, Oxford, 1962.